J. Phys. Chem. A **2008,** *112,* 12097–12103 **12097**

Generation and Dissociation Pathways of Singly and Doubly Protonated Bisguanidines in the Gas Phase

Aura Tintaru,[†,‡] Jana Roithová,[*,†,§] Detlef Schröder,[*,†] Laurence Charles,[‡] Iva Jušinski,[||] Zoran Glasovac,[||] and Mirjana Eckert-Maksić[*,||]

Institute of Organic Chemistry and Biochemistry, Flemingovo nám. 2, 16610 Prague 6, Czech Republic, Universités Aix-Marseille I, II et III - CNRS, UMR 6264, Laboratoire Chimie Provence, Equipe Spectrométries Appliquées à la Chimie Structurale, 13397 Marseille, France, Department of Organic Chemistry, Faculty of Sciences, Charles University in Prague, Hlavova 8, 12843 Prague 2, Czech Republic, and Division of Organic Chemistry and Biochemistry, Ruđer Bošković Institute, POB 180, HR-10002, Zagreb, Croatia

Received: July 4, 2008; Revised Manuscript Received: October 7, 2008

Para-bisguanidinyl benzene **1** and its *N*-permethylated derivative **2** are both sufficiently strong bases to afford not only the monocations $[\mathbf{1}+\mathrm{H}]^{+}$ and $[\mathbf{2}+\mathrm{H}]^{+}$, but also the doubly protonated ions, $[\mathbf{1}+2\mathrm{H}]^{2+}$ and $[\mathbf{2}+2\mathrm{H}]^{2+}$, in the gas phase. The title ions generated via electrospray ionization are probed by collision-induced dissociation experiments which inter alia reveal that the dicationic species $[\mathbf{1}+2\mathrm{H}]^{2+}$ and $[\mathbf{2}+2\mathrm{H}]^{2+}$ can even undergo fragmentation reactions with maintenance of the 2-fold charge. Complementary results from density functional theory predict PAs above 1000 kJ mol^{-1} for the neutral compounds, i.e., PA(**1**) = 1025 kJ mol^{-1} and PA(**2**) = 1067 kJ mol^{-1}. Due to the stabilization of the positive charge in the guanidinium ions and the para-phenylene spacer separating the basic sites, even the monocations bear sizable proton affinities, i.e., PA($[\mathbf{1}+\mathrm{H}]^{+}$) = 740 kJ mol^{-1} and PA($[\mathbf{2}+\mathrm{H}]^{+}$) = 816 kJ mol^{-1}.

Introduction

Guanidinium ions and related compounds are important structural motifs in organic and biological chemistry and prototypes of donor-stabilized carbenium ions. As a result of the large cation stabilities, the corresponding neutral guanidines are very basic compounds, often even superbases.[1-3] Inspired by recent work on the stability of medium-sized multiply charged ions,[4-6] we asked ourselves the question about the interaction of two spatially separated guanidinium ions in the gas phase. As a first approach in this direction, the bisguanidine model compounds **1** and **2** (Scheme 1) have been synthesized as the corresponding hydrochlorides.

Here, we describe the electrospray ionization (ESI) mass spectra of these compounds and the fragmentation patterns of the resulting mono- and dications generated from these samples. The experimental work is complemented by a theoretical determination of the first and second proton affinities of compounds **1** and **2** and an elucidation of the fragmentation pathways.

SCHEME 1: Structures of the Bisguanidines 1 and 2 Used As Precursors

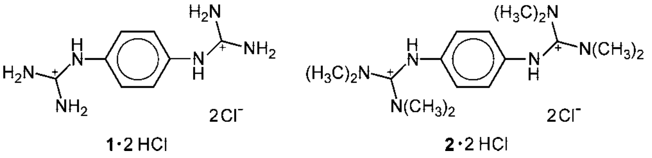

Experimental and Theoretical Methods

The experiments were performed with a Finnigan LCQ Classic ion-trap mass spectrometer which has newly been installed in the Prague laboratory. Because this is a commercial instrument with only a few technical modifications of the inlet system for the sprayed solution and an additional gas line for the introduction of neutral reagents into the ion trap, a brief description may suffice. The LCQ bears a conventional ESI source consisting of the spray unit (typical flow rate 5 μL/min., typical spray voltage 5 kV) with nitrogen as a sheath gas, followed by a heated transfer capillary (kept at 200 °C), a first set of lenses which determine the soft- or hardness of ionization by variation of the degree of collisional activation in the medium-pressure regime,[7,8] two transfer octopoles, and a Paul ion-trap for ion storage and manipulation[9] in the presence of ca. 10^{-5} mbar helium as a trapping gas. For detection, the ions are ejected from the trap to an electron multiplier. While the system is differentially pumped to ensure a smooth transition from atmospheric pressure to high vacuum, the relatively short distance (ca. 30 cm) of the ion trap from the spray needle in conjunction with the limited sophistication of the pumping system result in a considerable amount of the spray solvent (as well as nitrogen serving as the sheath gas) being present in the ion trap. Moreover, due to memory effects, notable amounts of previously used solvents (e.g., water, acetonitrile) may persist in the ion trap for extended periods of time. These contaminations to the helium do not affect the results on the guanidinium ions presented below, but make the interpretation of some of the labeling data more difficult because of H/D exchange with background protons(deuterons) occurring during the trapping and manipulation of ions; rapid ion/molecule reactions can even prevent the detection of reactive species in an ion trap.[10,11] Low-energy collision-induced dissociation (CID) was performed by application of an excitation AC voltage to the end caps of the trap to induce collisions of the isolated ions with the helium

---

[*] To whom correspondence should be addressed.

[†] Institute of Organic Chemistry and Biochemistry.

[‡] Universités Aix-Marseille I, II et III.

[§] Charles University in Prague.

[||] Ruđer Bošković Institute.

10.1021/jp805897f CCC: $40.75

SCHEME 2: Primary Pathways in the Fragmentation of the Monocation [1+H]$^{+a}$

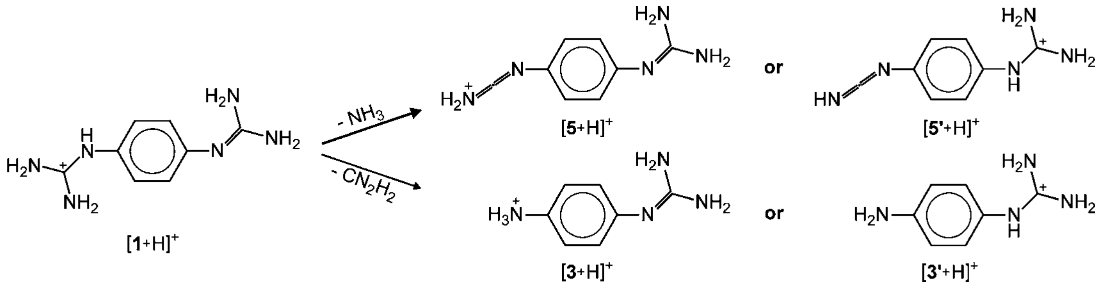

[a] The major route is highlighted by a bold arrow.

buffer gas for a period of 100 ms. While the CID energies can be varied continuously and also schemes for the conversion into threshold energies have been proposed,[12] we refrain from an exact quantification here and rather refer to them as a percentage of the 2.5 V excitation voltage applied. A more reliable description of the energetics is instead provided by the theoretical studies reported below. Likewise, with regard to the proton affinities of the monocations we rely on the calculated values, because the experimental determination of second proton affinities using techniques like the kinetic method is hampered by the intrinsic kinetic barrier resulting from Coulomb repulsion of the pair of monocationic fragments formed,[13,14] and a quantitative analysis would require a priori vague estimation of the charge-separation barrier,[15] whereas the computational prediction of gas-phase proton affinities has reached a high level of accuracy.[16]

The calculations employed the hybrid density functional method B3LYP[17] with the 6-311++G(2d,p) basis sets as implemented in Gaussian 03.[18] For the conversion from 0 K data to thermochemical properties at 298 K, the unscaled frequencies were used in conjunction with $\Delta H_g(H^+) = 6.2$ kJ mol^{-1} and $\Delta G_g(H^+) = -26.1$ kJ mol^{-1} for the free proton. Because theory tends to slightly overestimate absolute proton affinities, the gas-phase proton affinities reported below were scaled according to the recommendations of Hwang et al.[16] as $PA_{298,\text{scaled}} = (PA_{298,\text{th}} + 27.75 \text{ kJ mol}^{-1})/1.0588$ for this combination of method and basis set. Based on previous experience,[19] this empirical approach may well suffice as a first order compromise between required accuracy and computational demands. Further, most of the energetics are derived from isodesmic proton-transfer reactions in which many errors are expected to cancel each other.[20]

The bis-guanidinium dihydrochlorides **1**·2 HCl and **2**·2 HCl were prepared according literature procedures[21,22] starting from commercially available 1,4-phenylene diamine dihydrochloride and 1,4-phenylene diamine, respectively. The solvents were dried over magnesium ethoxide (ethanol) and calcium hydride (benzene) while other starting materials were used without additional purification. All reactions were conducted under inert atmosphere. NMR data for the bis-guanidinium salt **1**·2 HCl: ^{1}H NMR (DMSO-d$_6$, TMS, δ/ppm): 7.29 (s, 4H), 7.59 (s, 8H), 10.27 (s, 2H); ^{13}C NMR (DMSO-d$_6$, TMS, δ/ppm):126.8, 133.9, 156.9. The ^{1}H and ^{13}C NMR data for **2**·2 HCl agree with the literature data given in ref 22.

Results and Discussion

Electrospray ionization (ESI) of a methanolic solution of **1**·2 HCl under mild ionization conditions gives rise to the singly and doubly protonated molecules [**1**+H]$^+$ (*m*/*z* 193) and [**1**+2H]$^{2+}$ (*m*/*z* 97), respectively, with a ratio of about 1:2, as the by far dominating signal of the ESI mass spectra. To a small extent, also some daughter ions are observed in the source spectra which can be accounted for by the fragmentation sequences discussed below. Within a period of about half an hour, however, a considerable amount of solvolysis of the guanidinum salts is observed, as recognized by notable signals at *m*/*z* 151 and 109, which are attributed to the *N*-(aminophenyl)-guanidinium ion [**3**+H]$^+$ and protonated 1,4-phenylene diamine [**4**+H]$^+$, respectively. The major fragmentation pathway upon collision-induced dissociation (CID) of mass-selected [**1**+H]$^+$ corresponds to a loss of neutral ammonia (*m*/*z* 176) which is assigned to a formal 1,2-elimination leading to species [**5**+H]$^+$ or its tautomer [**5′**+H]$^+$ (Scheme 2). A minor route leads to a loss of a neutral molecule with mass 42. Given the elemental composition of the precursor, the neutral is assigned to CH_2N_2, either cyanamide (H_2NCN) or carbodimide (HNCNH),[23,24] which have very similar stabilities and are both conceivable to be formed from [**1**+H]$^+$ by 2-fold proton transfer from the terminal amino groups concomitant with CN bond cleavage to afford the cation [**3**+H]$^+$ or the tautomer [**3′**+H]$^+$. The nontrivial aspect of tautomeric forms of the fragment ions is addressed further below by reference to the computational results.

SCHEME 3: Primary Pathways in the Fragmentation of the Dication [1+2H]$^{2+a}$

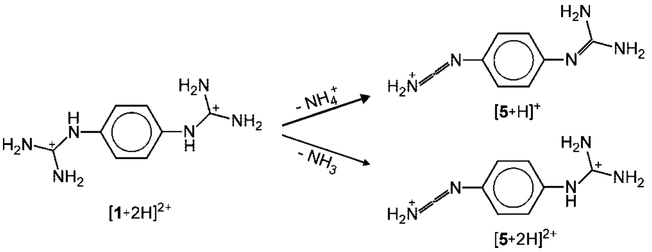

[a] The major route is highlighted by a bold arrow.

CID of the dication [**1**+2H]$^{2+}$ leads to a loss of neutral ammonia [**5**+2H]$^{2+}$ (*m*/*z* 88.5) in competition with proton transfer to afford the monocation [**5**+H]$^+$ or the tautomer [**5′**+H]$^+$ (both, *m*/*z* 176), of which the charge-separation pathway largely predominates (ca. 20:1 depending on collision energy). Hence, the Coulomb repulsion of the cationic centers in [**1**+2H]$^{2+}$ is sufficiently small to allow the formation of the long-lived dication in the gas phase, but occurrence of proton transfer is preferred in the course of the elimination of ammonia and leads to charge separation concomitant with formation of two monocations (Scheme 3).

Attempts to exchange the amino-protons of **1** by deuterium were of limited success. Thus, when using D_2O as a solvent, rapid hydrolysis of the guanidinum units in solution leads to [D$_4$-**4**+D]$^+$ (*m*/*z* 114) as the largely predominating ion upon ESI. With CD_3OD as a solvent, the signals for [**1**+H]$^+$ (*m*/*z*

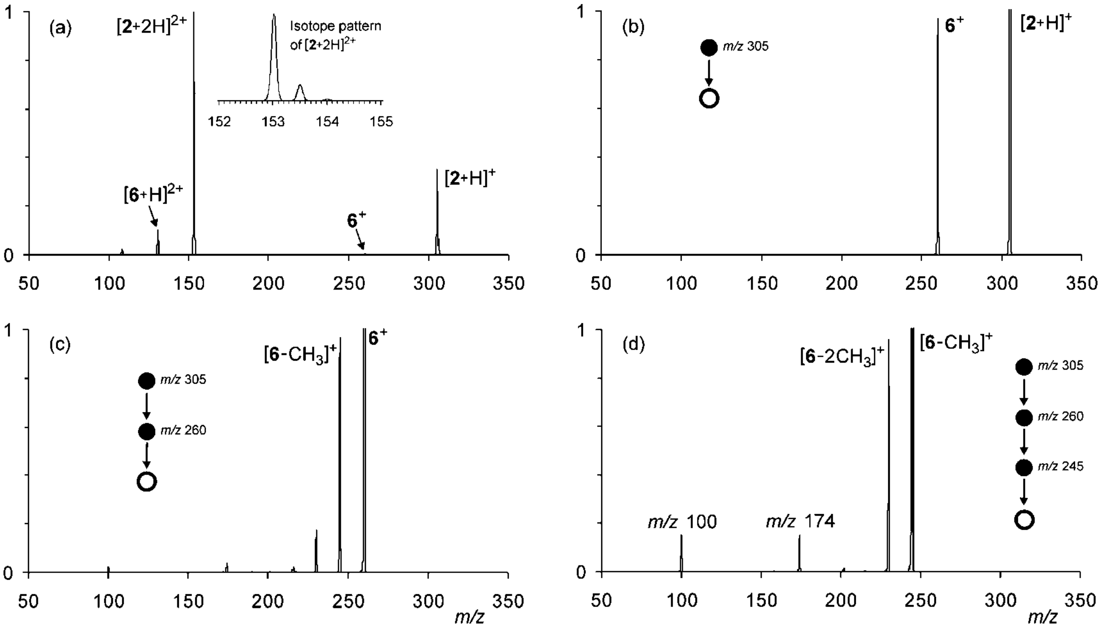

Figure 1. Selected mass spectra of compound **2**. (a) ESI mass spectrum of **2**$\cdot$ HCl showing the resulting monocation $[\mathbf{2}+\mathrm{H}]^+$ (*m*/*z* 305) as well as the dicationic species $[\mathbf{2}+2\mathrm{H}]^{2+}$ (*m*/*z* 153) as most abundant signals. In addition, small amounts of fragmentation (e.g., $\mathbf{6}^+$ and $[\mathbf{6}+\mathrm{H}]^{2+}$, *m*/*z* 260 and 130.5, respectively) are already occurring in the spray process. The inset show the isotope pattern of $[\mathbf{2}+2\mathrm{H}]^{2+}$ measured at enhanced mass resolution ("zoom-scan" option of the LCQ). (b) CID of mass-selected $[\mathbf{2}+\mathrm{H}]^+$ (*m*/*z* 305; 25% of the full collision amplitude) leads to $\mathbf{6}^+$ as exclusive fragment. (c) CID of mass-selected $\mathbf{6}^+$ (*m*/*z* 260; 30% of the full collision amplitude) generated from CID of mass-selected $[\mathbf{2}+\mathrm{H}]^+$ (27% of full collision energy) promotes fragments with $\Delta m = -15n$ ($n = 1 - 3$). (d) MS^4 experiment: CID of $[\mathbf{6}\text{-}\mathrm{CH_3}]^+$ (*m*/*z* 245; 20% of the full collision amplitude), generated by CID of mass-selected $\mathbf{6}^+$ (35% of the full collision amplitude), generated from CID of mass-selected $[\mathbf{2}+\mathrm{H}]^+$ (27% of full collision energy), shows a loss of a methyl radical ($\Delta m = -15$) and additional fragment ions at *m*/*z* 100 and 174. The former is assigned to the radical cation of bis(dimethylamino)carbene, $[(\mathrm{CH_3})_2\mathrm{N}]_2\mathrm{C}^{+\bullet}$, whereas the latter could have several origins (e.g., loss of $\mathrm{CH_3}$ followed by loss of $\mathrm{CH_3NCNH}$). In all MS^n experiments, the parent ions are off-scale (factors 6.5, 3.0, and 8.3 in panels b−d, respectively). The sequence of the MS/MS spectra also demonstrate the unique performance of IT-MS for MS^n experiments.[9]

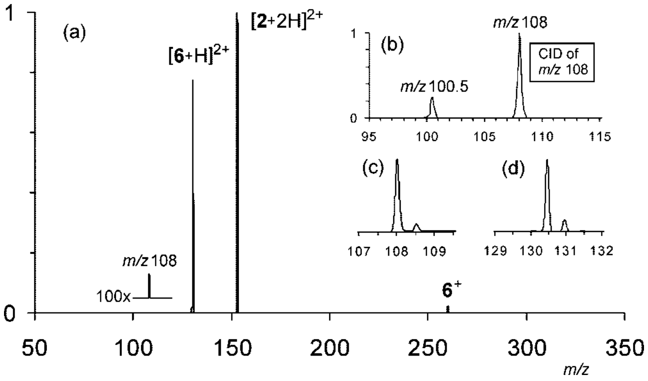

Figure 2. (a) CID mass spectrum of mass-selected $[\mathbf{2}+2\mathrm{H}]^{2+}$ (*m*/*z* 153, 15% of full collision energy) showing the competing losses of neutral dimethylamine to afford the dicationic species $[\mathbf{6}+\mathrm{H}]^{2+}$ (*m*/*z* 130.5) and of ammonium ion concomitant with production of the monocation $[\mathbf{6}]^+$ (*m*/*z* 260). The weak consecutive fragment at *m*/*z* 108 is also shown with 100-fold amplification and a vertical offset. (b) MS^4 experiment: CID of mass-selected *m*/*z* 108 (15% of full collision energy) generated from mass-selected $[\mathbf{6}+\mathrm{H}]^{2+}$ (*m*/*z* 130.5, 50% of full collision energy) generated from $[\mathbf{2}+2\mathrm{H}]^{2+}$ (*m*/*z* 153, 50% of full collision energy) showing the loss of a neutral methyl radical from the dicationic species to afford a fragment dication with *m*/*z* 100.5. (c) Isotope pattern of *m*/*z* 108 measured at enhanced mass resolution; the $^{13}\mathrm{C}$ pattern with half-masses unambiguously identifies the fragment as a dication. (d) Isotope pattern of $[\mathbf{6}+\mathrm{H}]^{2+}$ measured at enhanced mass resolution; the $^{13}\mathrm{C}$ pattern with half-masses unambiguously identifies the fragment as a dication.

193) and $[\mathbf{1}+2\mathrm{H}]^{2+}$ (*m*/*z* 97) shift to *m*/*z* 202 and 102, respectively, corresponding to the deuterated species $[\mathrm{D_8}\text{-}\mathbf{1}+\mathrm{D}]^+$ and $[\mathrm{D_8}\text{-}\mathbf{1}+2\mathrm{D}]^{2+}$ with all amino-hydrogen atoms being exchanged by deuterium. Within a period of only several minutes, however, the isotope patterns broaden indicating the occurrence of subsequent exchange processes which also involve the ring protons; in addition, hydrolysis with residual water in the inlet system took place. Given the speed of the subsequent exchange-reactions, more extensive MS/MS experiments with the deuterated compound were therefore considered to be of limited significance and thus not pursued any further.

Similar to **1**, the ESI spectra of the *N*-permethylated compound **2** dissolved in water yields intense signals for $[\mathbf{2}+\mathrm{H}]^+$ (*m*/*z* 305) and $[\mathbf{2}+2\mathrm{H}]^{2+}$ (*m*/*z* 153), respectively (Figure 1a). At low collision energies, CID of $[\mathbf{2}+\mathrm{H}]^+$ leads to an ion with *m*/*z* 260 as the exclusive fragment (Figure 1b) which corresponds to a loss of neutral dimethylamine ($\Delta m = -45$). At higher collision energies, additional fragments appear at *m*/*z* 215, 230, and 245 (not shown). An MS^3 experiment of the fragment ion with *m*/*z* 260 selected after CID of mass-selected *m*/*z* 305 (Figure 1c), reveals the signals at *m*/*z* 215, 230, and 245 as consecutive fragments of *m*/*z* 260, which may either correspond to sequential $\mathrm{CH_3}^\bullet$ losses ($\Delta m = -15n$ with $n = 1 - 3$) or the expulsion of an intact ethane molecule ($\Delta m = -30$) and a second dimethylamine unit ($\Delta m = -45$).

At the first sight, the loss of a methyl radical from *m*/*z* 260, a closed-shell ion, might appear to contradict with the even-electron rule,[28] but exceptions from this rule are indeed quite common in the case of protonated nitrogen bases.[29] As the product of the first $\mathrm{CH_3}^\bullet$ loss is a cation radical, a second loss of a radical might therefore occur even much easier;[30] by analogy, even $\Delta m = -45$ could correspond to the loss of three $\mathrm{CH_3}^\bullet$ radicals rather than intact dimethylamine. At least for $\Delta m = -30$, the MS^n experiments shown in Figure 1, panels c and d, demonstrate that sequential losses of two methyl radicals can occur for the ion with *m*/*z* 260. Due to the lack of additional information, e.g., MS^n spectra of appropriately labeled sub-

SCHEME 4: Primary Fragmentation Pathways of the Mono- and Diprotonated Species [2+H]$^+$ and [2+2H]$^{2+a}$

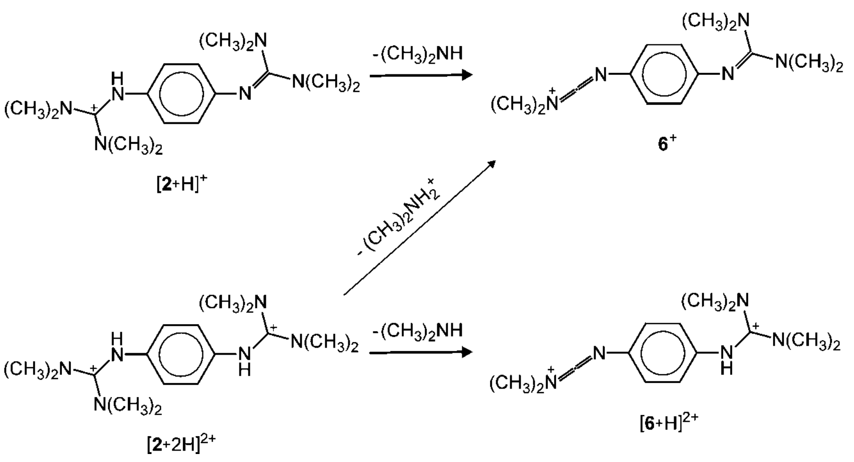

[a] Major routes are highlighted by bold arrows.

SCHEME 5: Fragmentation Pathways of the Singly Protonated Guanidine Base 1^a

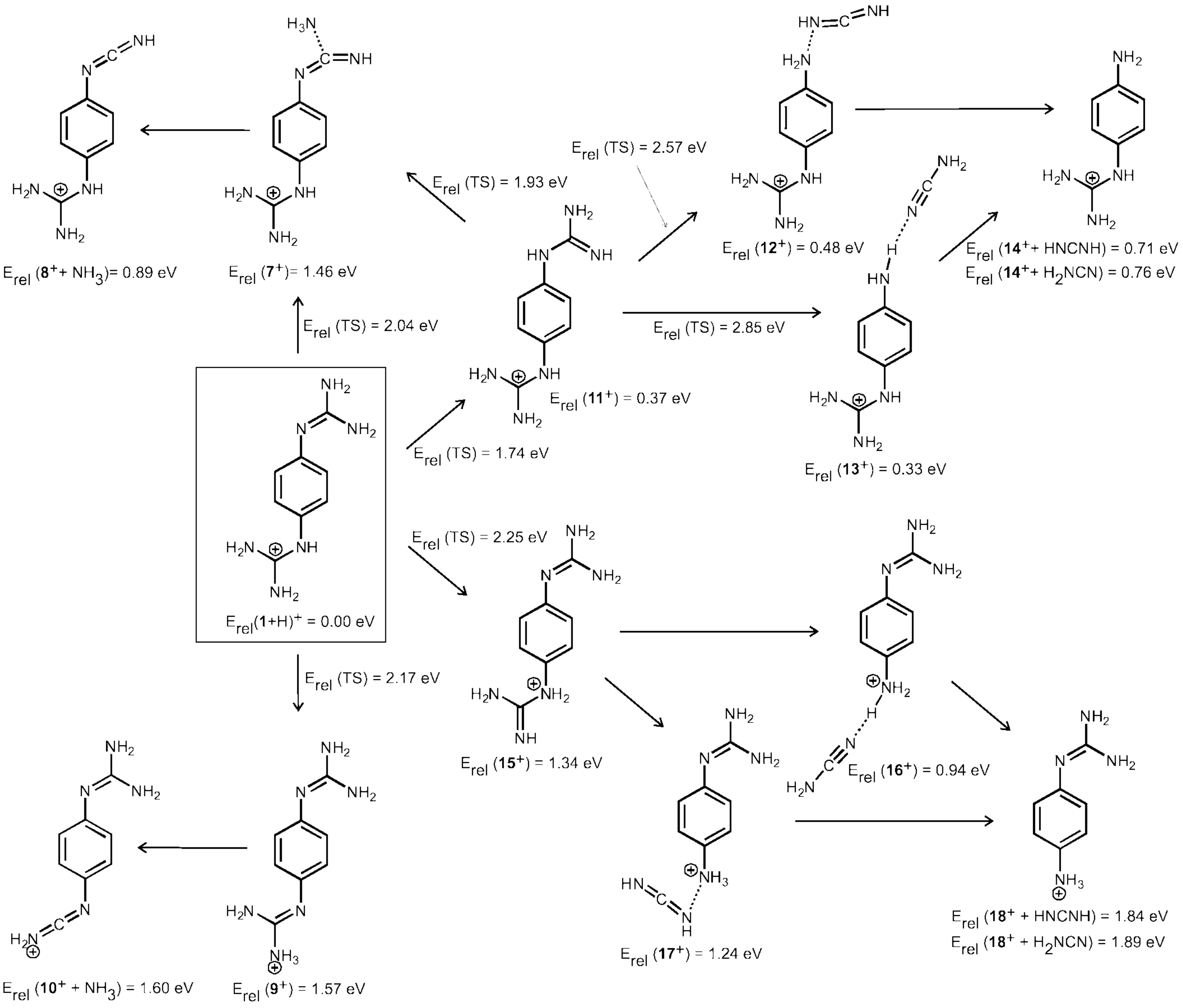

[a] Energies are given relative to energy of the parent ion [1+H]$^+$ at 0 K; $E_{0K}([1+H]^+) = -640.987571$ hartree.

strates, the structures of the fragments resulting from the consecutive losses of $CH_3^{\bullet}$ remain uncertain, however. We note further that when D_2O is used as solvent, CID of so-formed [**2**+D]$^+$ (*m*/*z* 306) leads to a loss of $\Delta m = -46$, corresponding to [*N*-D]-dimethylamine, and thus again affording the ion with *m*/*z* 260, as expected.

SCHEME 6: Fragmentation Pathways of the Doubly Protonated Guanidine Base 1[a]

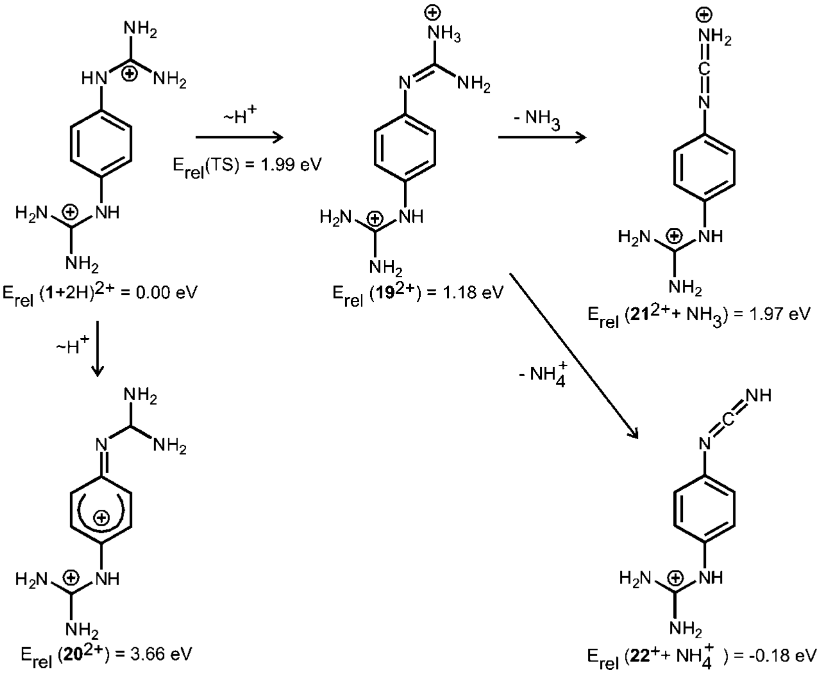

[a] Energies are given relative to energy of the parent ion $[\mathbf{1}+2H]^{2+}$ at 0 K; $E_{0K}([\mathbf{1}+2H]^{2+}) = -641.269534$ hartree).

CID of the dicationic species $[\mathbf{2}+2H]^{2+}$ (*m*/*z* 153, Figure 2a) leads to competing losses of neutral and protonated dimethylamine to afford a dicationic species with *m*/*z* 130.5 and the monocation with *m*/*z* 260 already described above. Interestingly, dication fragmentation with maintenance of the 2-fold charge prevails at all collision energies studied and at higher collision energies, even a second dimethylamine molecule is lost from the primary fragment to afford a dication with *m*/*z* 108. From the latter dication, even another radical moiety ($CH_3^{\bullet}$) can be lost upon CID without occurrence of Coulomb explosion (Figure 2b). Notably, the loss of a methyl radical upon successive CID parallels the demethylation observed for the monocationic species (see above), and hence the fragmentation sequence dication very much resembles that of the monocation.

ESI from D_2O solution affords a clean and complete labeling of the mobile protons, i.e., the dication $[\mathbf{2}+2D]^{2+}$ (*m*/*z* 154), whose CID yields the corresponding fragments with *m*/*z* 131 and 260, i.e., losses of neutral [*N*-D]-dimethylamine and the deuteronated amine, [*N*-D_2]-dimethylammonium, respectively. Note that the fragment at *m*/*z* 260 does no longer contain any deuterium and hence $(CH_3)_2ND_2^+$ is lost as a cation from $[\mathbf{2}+2D]^{2+}$; the ionic fragment $(CH_3)_2ND_2^+$ (*m*/*z* 46) is again not observed experimentally due to inefficient trapping of low mass ions in the ITMS. The fact that $(CH_3)_2ND_2^+$ evolves from $[\mathbf{2}+2D]^{2+}$ further demonstrates that both charge centers can to some extent “communicate” across the phenylene spacer (see below). In contrast to **1**, no notable amount of H/D exchange of the ring-protons of **2** is occurring in the deuterated solvent. The initial fragmentation sequences of $[\mathbf{2}+H]^+$ and $[\mathbf{2}+2H]^{2+}$ can accordingly be summarized in terms of Scheme 4.

The experimental results described above demonstrate that the guanidines **1** and **2** are both strong bases, as expected, and that even the nonsolvated doubly protonated forms can exist as isolated, long-lived species in the highly diluted gas phase. Of interest are thus their thermochemical properties which are elucidated with the help of calculations employing density functional theory.

The ab initio calculations reveal that the proton affinity of **1** amounts to $PA(\mathbf{1})_{0K} = 1025$ kJ mol^{-1} which increases to $PA(\mathbf{2})_{0K} = 1067$ kJ mol^{-1} for the *N*-permethylated compound. In addition, even the proton affinity of protonated $[\mathbf{1}+H]^+$ still reaches an appreciable value of $PA([\mathbf{1}+H]^+)_{0K} = 740$ kJ mol^{-1}, and for the *N*-permethylated analogue, the value increases to $PA([\mathbf{2}+H]^+)_{0K} = 816$ kJ mol^{-1}. These rather large values for the second proton affinities suggest that the charged sites of the dications $[\mathbf{1}+2H]^{2+}$ and $[\mathbf{2}+2H]^{2+}$ are sufficiently separated so that the mutual repulsion of the positive charges does not substantially destabilize the doubly protonated products.[31]

The fragmentation mechanisms are elucidated in more detail for the potential-energy surfaces of the singly and doubly protonated molecule **1**. The major fragmentation channel for $[\mathbf{1}+H]^+$ leads to elimination of ammonia, where the latter can be eliminated either from the protonated or from the neutral guanidinyl group in the molecule. According to the calculations (Scheme 5), the rearrangements within the neutral guanidinyl group involve slightly lower energy barriers compared to those processes involving the protonated moiety. Moreover, also the resulting product is more stable, if NH_3 is eliminated from the neutral guanidinyl group ($E_{rel}(\mathbf{8}^+ + NH_3) = 0.89$ eV) than from the charged site ($E_{rel}(\mathbf{10}^+ + NH_3) = 1.60$ eV), which also means that the PA of the guanidine unit is 0.71 eV larger than the PA of the carbodimide moiety. The second experimentally observed fragmentation pathway leads to the elimination of $[CN_2H_2]$, either cyanamide or carbodiimide (see above). The fragmentation is again energetically more favorable if the neutral guanidine group is involved, in that product $\mathbf{14}^+$ is by 1.13 eV more stable than $\mathbf{18}^+$. As expected, the eliminations of either NH_2CN or HNCNH are preceded by a series of hydrogen rearrangements, where the rate-determining steps are slightly higher than for the loss of ammonia, which is consistent with the experimental data. Once more, all isomers formed by a rearrangement within the neutral guanidinyl group are significantly more stable than those formed by a hydrogen migration within the guanidinium unit.

SCHEME 7: Hydrogen Rearrangements in the Doubly Protonated Guanidine Base [1+2H]$^{2+}$

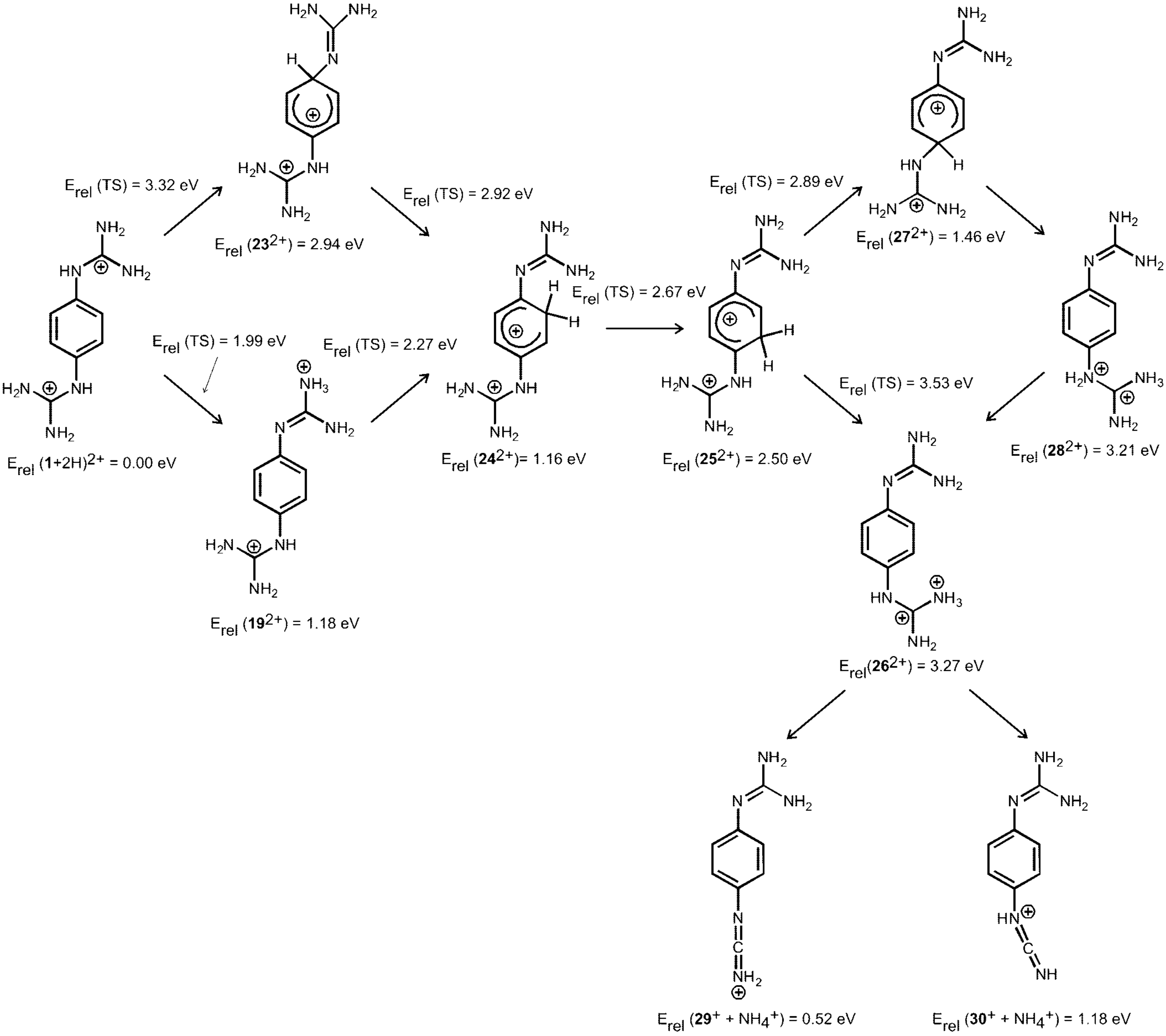

Hence, the dissociation of energized [**1**+H]$^{+}$ is an example for a charge-remote fragmentation.[32] The fact that fragmentation of the neutral nonactivated guanidine group is energetically preferred over the fragmentation of the protonated group is most probably related to the large stability of the guanidinium ion. Thus, rearrangement within the protonated group leads to a large destabilization of the cation and leads to final product **18**$^{+}$ bearing a proton at a site with lower proton affinity than the guanidine group. On the other hand, the fragmentation of the neutral part of the molecule conserves the favorable guanidinium structure and leads to more energetically favored product **14**$^{+}$.

The fragmentation of doubly protonated **1** is dominated by competition between losses of ammonium ion and neutral ammonia. The eliminations are preceded by a hydrogen migration between the nitrogen atoms of the guanidinium group to form isomer **19**$^{2+}$ (Scheme 6). The rearrangement is associated with an energy barrier of 1.99 eV, which is comparable to the values found for singly protonated molecule. In comparison, rearrangement of a hydrogen atom to the central carbon atom of the guanidinium group leads to an isomer with high internal energy, $E_{\rm rel}(\mathbf{20}^{2+}) = 3.66$ eV. The isomer **19**$^{2+}$ can either lose neutral ammonia, which however leads to a product with high relative energy ($E_{\rm rel}(\mathbf{21}^{2+} + \mathrm{NH_3}) = 1.97$ eV). If the fragmentation is coupled with proton transfer so that ammonium ion is eliminated, the resulting products lie much lower in energy ($E_{\rm rel}(\mathbf{22}^{+} + \mathrm{NH_4}^{+}) = -0.18$ eV), which accounts for the preference of this channel in the experiments.

The elimination of neutral dimethylamine from the *N*-permethylated dication [**2**+2H]$^{2+}$ most probably proceeds via an analogous mechanism. On the other hand, the elimination of the charged fragment, dimethylammonium ion, requires the migration of a proton from one hemisphere of the ion to the other. Such a mechanism involves a whole series of hydrogen rearrangements along the entire skeleton (“hydrogen ring walk”),[33] which leads over relatively high barriers, as demonstrated by exploratory calculations for the lighter analogue [**1**+2H]$^{2+}$. The results summarized in Scheme 7 indicate that the energy barriers for hydrogen migration around the aromatic ring largely exceed the energy demand for the loss of neutral ammonia, which means that such a process will be largely disfavored. By analogy, the same conclusions may be drawn for the loss of dimethylammonium from [**2**+2H]$^{2+}$ and we have therefore not explicitly studied the corresponding pathways for the *N*-permethylated derivative.

In addition to the ring-walk mechanism, an alternative scenario for the loss of dimethylammonium from $[\mathbf{2}+2\mathrm{H}]^{2+}$ evolves from consideration of the formation of an intermediate ion/neutral complex.[31] Here, this scenario would correspond to a loosely bound adduct of $[\mathbf{6}+\mathrm{H}]^{2+}$ with neutral dimethylamine (see Scheme 4). In such a complex, the only electrostatically bound amine could migrate in the outer sphere from one terminus of the molecule to the other and thereby bypass the need for hydrogen-ring walk. A characteristic of such a mechanism is, however, the relatively weak interaction of the fragments with each other such that we have not undertaken any attempts to localize such ion/neutral complexes using density functional theory.[35] Given the fact that the PA of dimethylamine (930 kJ mol^{-1})[36] even exceeds PA($[\mathbf{2}+\mathrm{H}]^{+}$) = 816 kJ mol^{-1}, involvement of an ion/neutral complex in the charge-separation reaction of $[\mathbf{2}+2\mathrm{H}]^{2+}$ does in fact appear quite likely.

Conclusions

The present ESI-MS studies of the bisguanidines **1** and **2** demonstrate that these two compounds are indeed suitable models for the investigation of the perturbation of two distant, but still interacting charges in a doubly protonated closed-shell molecules. Thus, both compounds exhibit sizable second proton affinities (740 and 816 kJ mol^{-1}, respectively), and at least for the permethylated compound **2**, the doubly protonated form $[\mathbf{2}+2\mathrm{H}]^{2+}$ exhibits a fragmentation scheme on the dication surface which very much resembles that of the monocation $[\mathbf{2}+\mathrm{H}]^{+}$, i.e., first loss(es) of dimethylamine, then expulsion of methyl radicals. Accordingly, compound **2** appears as a promising candidate for future attempts to realize cation/cation reactions, i.e., protonation of the monocation $[\mathbf{2}+\mathrm{H}]^{+}$ in the ion/molecule reaction with a strong Brønsted acid AH^{+}.[37,38]

Acknowledgment. This work was supported by the Grant Agency of the Czech Republic (203/08/1487), the Czech Academy of Sciences (Z40550506), the Ministry of Education of the Czech Republic (MSM0021620857), and the Ministry of Science, Education, and Sport of Croatia (098-0982933-2920).

References and Notes

(1) Alder, R. W. *J. Am. Chem. Soc.* **2005**, *127*, 7924.

(2) Kovačević, K.; Maksić, Z. B. *Chem. Commun.* **2005**, 1524.

(3) (a) Glasovac, Z.; Štrukil, V.; Eckert-Maksić, M.; Schröder, D.; Kacorowska, M.; Schwarz, H. *Int. J. Mass Spectrom.* **2008**, *270*, 39. (b) Eckert-Maksić, M.; Glasovac, Z.; Trošelj, P.; Kütt, A.; Rodima, T.; Koppel, T.; Koppel, I. A. *Eur. J. Org. Chem.* **2008**, 5176.

(4) Schröder, D.; Schwarz, H. *J. Phys. Chem. A* **1999**, *103*, 7385.

(5) Schröder, D. *Angew. Chem., Int. Ed.* **2004**, *43*, 1329.

(6) Roithová, J.; Schröder, D. *Phys. Chem. Chem. Phys.* **2007**, *9*, 2341.

(7) Cech, N. B.; Enke, C. G. *Mass Spectrom. Rev.* **2001**, *20*, 362.

(8) (a) Schröder, D.; Weiske, T.; Schwarz, H. *Int. J. Mass Spectrom.* **2002**, *219*, 729. (b) Trage, C.; Diefenbach, M.; Schröder, D.; Schwarz, H. *Chem. Eur. J.* **2006**, *12*, 2454.

(9) O'Hair, R. A. J. *Chem. Commun.* **2006**, 1469.

(10) Jagoda-Cwiklik, B.; Jungwirth, P.; Rulíšek, L.; Milko, P.; Roithová, J.; Lemaire, J.; Maitre, P.; Ortega, J. M.; Schröder, D. *ChemPhysChem* **2007**, *8*, 1629.

(11) Milko, P.; Roithová, J.; Schröder, D.; Lemaire, J.; Schwarz, H.; Holthausen, M. C. *Chem. Eur. J.* **2008**, *14*, 4318.

(12) (a) Colorado, A.; Brodbelt, J. *J. Am. Soc. Mass Spectrom.* **1996**, *7*, 1116. (b) Waters, T.; O'Hair, R. A. J.; Wedd, A. G. *J. Am. Chem. Soc.* **2003**, *125*, 3384. (c) O'Hair, R. A. J.; Vrkic, A. K.; James, P. F. *J. Am. Chem. Soc.* **2004**, *126*, 12173. (d) Khairallah, G. N.; O'Hair, R. A. J. *Angew. Chem., Int. Ed.* **2005**, *44*, 728.

(13) Gronert, S. *J. Mass Spectrom.* **1999**, *34*, 787.

(14) (a) Viggiano, A. A., Dressler, R. A. In *The Encyclopedia of Mass Spectrometry*; Nibbering, N. M. M., Ed.; Elsevier: Oxford, U.K., 2005; Vol. 4, p 542. (b) McLuckey, S. A. In *The Encyclopedia of Mass Spectrometry*; Nibbering, N. M. M., Ed.; Elsevier: Oxford, U.K., 2005; Vol. 4, p 552. p. 552.

(15) (a) Petrie, S.; Javahery, G.; Wincel, H.; Wang, J.; Bohme, D. K. *J. Am. Chem. Soc.* **1993**, *115*, 6290. (b) Petrie, S.; Javahery, G.; Bohme, D. K. *Int. J. Mass Spectrom. Ion Processes* **1993**, *124*, 145.

(16) Hwang, S.; Jang, Y. H.; Chung, D. S. *Bull. Korean Chem. Soc.* **2005**, *26*, 585.

(17) (a) Becke, A. D. *J. Chem. Phys.* **1993**, *98*, 5648. (b) Vosko, S. H.; Wilk, L.; Nusair, M. *Can. J. Phys.* **1980**, *58*, 1200. (c) Lee, C.; Yang, W.; Parr, R. G. *Phys. Rev. B* **1988**, *37*, 785. (d) Miehlich, B.; Savin, A.; Stoll, H.; Preuss, H. *Chem. Phys. Lett.* **1989**, *157*, 200.

(18) *Gaussian 03*, revision C.02; Gaussian, Inc.: Wallingford, CT, 2004.

(19) Roithová, J.; Schröder, D.; Míšek, J.; Stará, I. G.; Starý, I. *J. Mass Spectrom.* **2007**, *42*, 1233.

(20) Roithová, J.; Exner, O. *J. Phys. Org. Chem.* **2001**, *14*, 752.

(21) Braun, C. E.; Erit, J. D.; Crooks, G. C. *J. Org. Chem.* **1938**, *3*, 146.

(22) Leffek, K. T.; Pruzynski, P.; Thanapaalasingham, K. *Can. J. Chem.* **1989**, *67*, 590.

(23) Tordini, F.; Bencini, A.; Bruschi, M.; De Gioia, L.; Zampella, G.; Fantucci, P. *J. Phys. Chem. A* **2003**, *107*, 1188.

(24) Duvernay, F.; Chiavassa, T.; Borget, F.; Aycard, J.-P. *J. Phys. Chem. A* **2005**, *109*, 603.

(25) Otto, M.; Conjero, S.; Canac, Y.; Romanenko, V. D.; Rudzetvitch, V.; Bertrand, G. *J. Am. Chem. Soc.* **2004**, *126*, 1016.

(26) Magill, A. M.; Cavell, K. J.; Yates, B. F. *J. Am. Chem. Soc.* **2004**, *126*, 8717.

(27) See also. McGibbon, G. A.; Terlouw, J. K. *Chem. Phys. Lett.* **1994**, *222*, 129.

(28) Thurmann, E. M.; Ferrer, I.; Pozo, O. J.; Sancho, J. V.; Hernandez, F. *Rapid Commun. Mass Spectrom.* **2007**, *21*, 3855.

(29) Levsen, K.; Schiebel, H. M.; Terlouw, J. K.; Jobst, K. J.; Elend, M.; Preib, A.; Thiele, H.; Ingendoh, A. *J. Mass Spectrom.* **2007**, *42*, 1024.

(30) Schröder, D.; Roithová, J.; Gruene, P.; Schwarz, H.; Mayr, H.; Koszinowski, K. *J. Phys. Chem. A* **2007**, *111*, 8925.

(31) A rough estimate of the role of Coulomb repulsion in the lowering of the second PA compared to the first can be obtained by determination of the average distance of the charge centers in the two bisguanidinium ions from the computed partial charges.[13] For $[\mathbf{1}+2\mathrm{H}]^{2+}$, in which the charge is mostly concentrated on the guanidine-carbon atom with some contributions from the NH_2 groups, the distance of the averaged charge centers amounts to $r = 8.4$ Å (compared to $r = 7.53$ Å of the two guanidine-carbon atoms), which results in a lowering of the PA by 1.70 eV only by the effect of Coulomb repulsion. In the case of compound $[\mathbf{2}+2\mathrm{H}]^{2+}$, in which the charge is mostly concentrated on the *N*-methyl groups, the distance of the averaged charge centers is larger $r = 9.3$ Å (while $r = 7.51$ Å between the two guanidine-carbon atoms is almost identical to $[\mathbf{1}+2\mathrm{H}]^{2+}$), resulting in a lowered Coulomb repulsion term of only 1.54 eV. The simplistic approach provides a qualitative rationale for the lower difference of the first and second PAs of **2** (ΔPA = 251 kJ mol^{-1}) compared to those of **1** (ΔPA = 285 kJ mol^{-1}), but fails quantitatively because through-bond repulsion via polarization as well as resonance effects are entirely neglected in this simplistic electrostatic approach.

(32) Cheng, C. F.; Gross, M. L. *Mass Spectrom. Rev.* **2000**, *19*, 398.

(33) (a) Kuck, D. *Mass Spectrom. Rev.* **1990**, *9*, 583. (b) Kuck, D. *Int. J. Mass Spectrom.* **2002**, *213*, 101.

(34) Longevialle, P. *Mass Spectrom. Rev.* **1992**, *11*, 157.

(35) For an elaborate discussion of the concept of ion/neutral complexes, their classification, and the difficulties to locate loosely bound intermediates computationally, see: Morton, T. H. In *The Encyclopedia of Mass Spectrometry*; Nibbering, N. M. M., Ed.; Elsevier, Oxford, U.K., 2005; Vol. 4, p 542.

(36) Taken from: NIST Standard Reference Database Number 69; NIST: Gaithersburg, 2005, see: http://webbook.nist.gov/chemistry/.

(37) See also: (a) Schröder, D.; Harvey, J. N.; Schwarz, H. *J. Phys. Chem. A* **2000**, *104*, 11257.

(38) Unfortunately, the software of the LCQ does not allow the simultaneous mass-selection of two ions, but there are no principal restrictions to such an approach.

JP805897F